AENSI Journals

Australian Journal of Basic and Applied Sciences

ISSN:1991-8178

Journal home page: www.ajbasweb.com

A Simplified Vector Based V/f method for CSI Fed 3Phase IM Drive Capable of High Performance Regulation at Wide Range of Speeds

[1]M. Arul Prasanna, [2]DR. V. Rajasekaran, [3]DR. I. Gerald Christopher Raj, [4]N. Panneer Selvam

[1]Assistant Professor, Department of EEE, PSNA College of Engineering & Technology, Dindigul, India.
[2]Professor & Head, Department of EEE, PSNA College of Engineering & Technology, Dindigul, India,
[3]Associate Professor, Department of EEE, PSNA College of Engineering & Technology, Dindigul, India.
[4]Assistant Professor, Department of EEE, Vickram College of Engineering & Technology, Sivaganga India.

ARTICLE INFO

Article history:
Received 12 January 2014
Received in revised form 5 March 2014
Accepted 8 March 2014
Available online 31 March 2014

Keywords:
Induction Motor, Vector control, VSI, CSI, V/f, MATLAB / Simulink

ABSTRACT

This Paper presents a simplified computer program for the simulation of CSI fed 3-Phase IM drive controlled by means of vector based V/f control method using MATLAB/SIMULINK simulation software. The main features of this type of simulation program are simplicity, accuracy and efficiency in terms of computation time. This simulation program can be used to verify the system design, to study system dynamic behavior and to investigate steady state waveforms of the drive system. The feasibility, reliability of the system and the validity of the control method are proved by the simulation results. The CSI drive has so many features compared to VSI drives. In addition, symmetrical GTO, when used as switching device in the CSI, makes the drive particularly suitable for implementation at medium high voltage (4160V and up) levels and also can be useful for wide range of speed control applications(from below to above rated speed).

To Cite This Article: M. Arul Prasanna, DR. V. Rajasekaran , DR. I. Gerald Christopher Raj , N. Panneer Selvam., A Simplified Vector Based V/f method for CSI Fed 3Phase IM Drive Capable of High Performance Regulation at Wide Range of Speeds. ***Aust. J. Basic & Appl. Sci.,*** *8(3): 151-160, 2014*

INTRODUCTION

Compared with voltage source inverter fed drives, the CSI drive has the features of simple structure, reliable short circuit protection, four quadrant operation capability and nearly sinusoidal output voltage and current waveforms. In addition, the switching device (symmetrical GTO) used in the CSI can be easily connected in series, which makes the CSI drive particularly suitable for implementation at medium high voltage (4160V and up) levels. Therefore a block diagram of the GTO CSI fed IM drive system is shown in Fig. 1. It is replacing the conventional Current Source Inverter drive in high power applications Ahmet (1999) & Aleksandar (2004).

To date, most simulation work for this type of drive system is carried out on a steady state basis Aleksandar (2008), Alfredo (1998), Babaei (2010) & Bimal K. Bose (2002). It is difficult to use general purpose simulation programs such as EMTP (Electromagnetic Transient Program) and SPICE (Simulation Program with Integrated Circuit Emphasis) to simulate the dynamic performance of the drive system due to the special PWM techniques employed in the inverter and the complicated IM model. However the MATLAB/Simulink software simulation tool is specially conceived for the development of continuous and discrete control systems. The main disadvantage of MATLAB/Simulink software is the one of not being specific software for power electronic systems and, therefore, the designer must develop his own models for electronic systems. A toolbox of Simulink named power system blockset is especially dedicated to the power electronic systems, although for a fixed structure is not as versatile as user defined models (s-functions). Nevertheless, the power stages topologies are fixed and well defined as opposed to the great amount of possibilities of control that offers a digital system (DSP), for a same power stage.

This Paper consists 4 sections. These sections elaborately describe the d-q axes model of IM with flux linkages as state variables especially for stability studies. The different drive sections which include rectifier section, CSI-IM section and control section are presented in detail. The simulation procedures, results are discussed. The dynamic performance of the drive system is presented in tabular form.

Corresponding Author: M. Arul Prasanna, Assistant Professor, Department of EEE, PSNA College of Engineering & Technology, Dindigul-624622, Tamilnadu, India.
Phone: +91 9944752376, E-Mail: arulresearch2006@gmail.com

2. CSI Fed Induction Motor Drive:

This section describes the main components involved in the control of Current source Inverter fed 3phase Induction motor drive such Rectifier Section, IM Drive System, Control Section and V/F control Mechanism in detail.

2.1 Control Block Diagram of CSI Fed IM Drive System

The control block diagram of the CSI fed IM drive system is shown in Figure 1. The drive system has a number of prominent features such as simple structure and sinusoidal outputs, and therefore it replaces the conventional CSI drive in medium to high power applications. In this paper, a specially designed computer simulation program is developed for the drive system shown below. In the program, the above drive system is divided into three sections: rectifier section, CSI-IM section and control section.

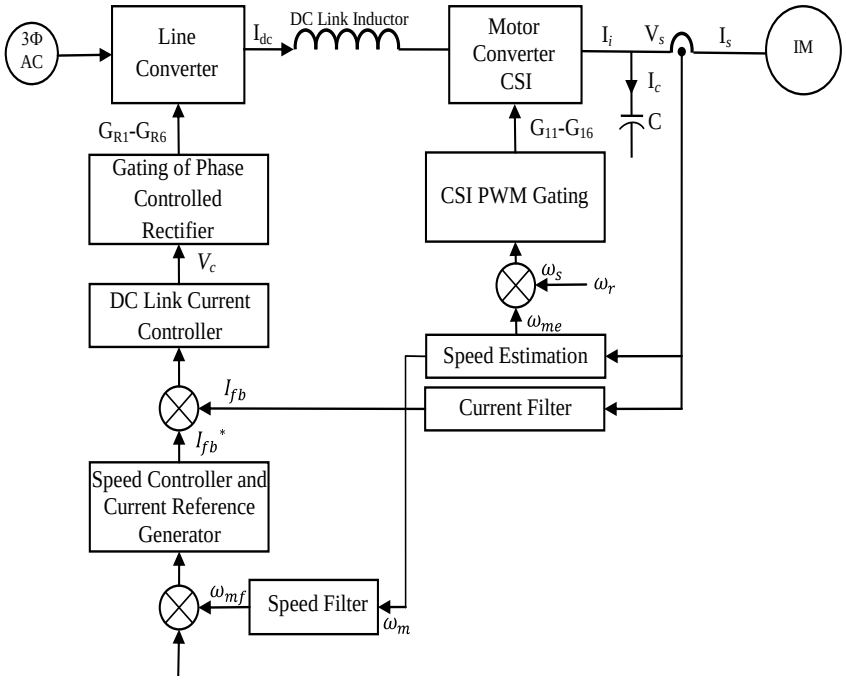

Fig. 1: Control Block Diagram of CSI Fed IM Drive System.

In general, switching of the power electronic switches in the power circuit increases the complexity for simulation. To simplify the simulation process, different simulation algorithms are developed for different sections.

2.2 Rectifier Section:

Figure 2 shows a simplified circuit diagram of a 3ϕ thyristor rectifier (line converter block of Figure.1. Since the effect of snubber circuits on the drive system performance is trivial, the snubber circuits are not considered in the simulation. It is also assumed that the line inductance between power supply and rectifier is zero, implying negligible DC voltage losses caused by the commutation of thyristors. Under these assumptions, the dc voltage waveform of the rectifierv_{dc} is defined only by the input voltage, the delay angle $\alpha$of gating pulses, and the continuity of dc link currenti_{dc}. Therefore, the simulation for the operation of the rectifier is straightforward and no numerical integration is required.

In this Paper a New MATLAB function program is developed for the rectifier section. The parameters passed to the program are RMS value of the line voltageV_{AB}, time instantt, delay angle αand DClink current i_{dc}.The program brings back the instantaneous value of the dc link voltagev_{dc}. The typical output waveforms are obtained from simulations, for continuous dc link current at the delay angles $\alpha = 0^{\circ}$, $\alpha = 30^{\circ}$and discontinuous dc link current at $\alpha = 75^{\circ}$ are illustrated in Figure 3.

2.3 CSI -IM Drive Section:

A circuit diagram of the CSI-IM section is shown in Figure 4.This section includes a dc link inductor, a CSI, 3ϕ output capacitor and an IM. Two commonly used modulation techniques, the trapezoidal pulse width modulation (TPWM) and the selected harmonic elimination (SHE) techniques **a**re considered in the program. According to Bin wu *et al* , six distinct states can be defined for the modulation patterns.

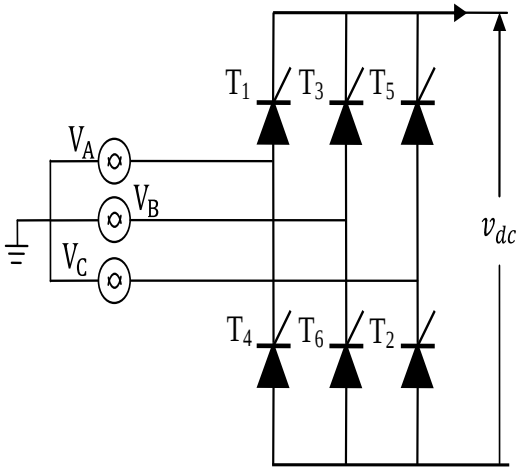

Fig. 2: Simplified Circuit Diagram of the Thyristor Rectifier.

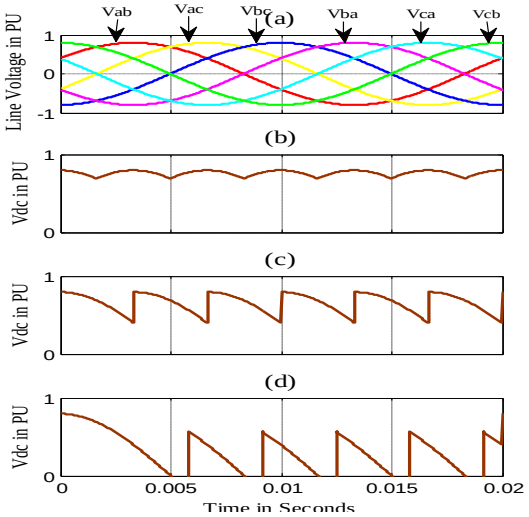

Fig. 3: Typical rectifier waveforms (a) Input line voltages for 50 Hz, Output voltages (b) at $\alpha = 0^{\circ}$ (c) at $\alpha = 30^{\circ}$(d) at $\alpha = 75^{\circ}$.

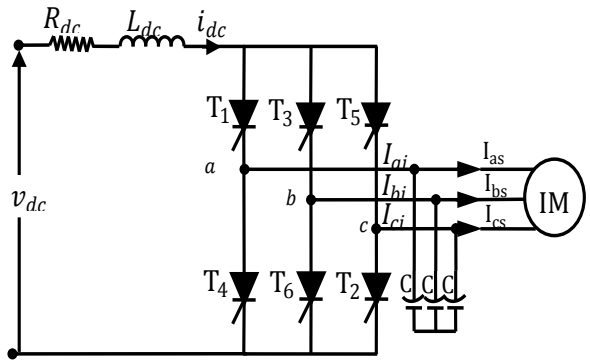

Fig. 4: Circuit diagram for the inverter-motor section.

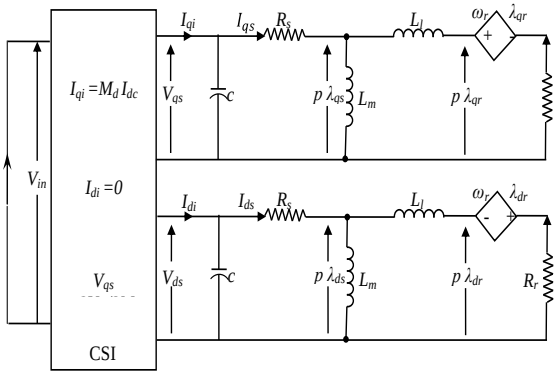

Fig. 5: Equivalent circuit of CSI-IM section.

The equivalent circuit for the CSI, capacitor and IM in a d-q axis rotating reference frame is shown in Figure 5. The corresponding state equation (differential equations) with motor flux linkages as variables is derived from Bin Wu (1994).

$$\dot{x} = Ax + Bu \tag{1}$$

Where $\dot{x} = \frac{dx}{dt}$

$$A = \begin{bmatrix} -\frac{R_s}{\sigma_m L_m} & 0 & \frac{R_s}{L_l} & 0 & 1 & 0 & 0 & 0 \\ 0 & -\frac{R_s}{\sigma_m L_m} & 0 & \frac{R_s}{L_l} & 0 & 1 & 0 & 0 \\ \frac{R_r}{L_l} & 0 & -\frac{R_r}{L_l} & \omega_{me} & 0 & 0 & 0 & 0 \\ 0 & \frac{R_r}{L_l} & -\omega_{me} & -\frac{R_r}{L_l} & 0 & 0 & 0 & 0 \\ -\frac{1}{\sigma_m L_m C} & 0 & \frac{1}{L_l C} & 0 & 0 & 0 & K(1) & 0 \\ 0 & -\frac{1}{\sigma_m L_m C} & 0 & \frac{1}{L_l C} & 0 & 0 & K(2) & 0 \\ 0 & 0 & 0 & 0 & K(3) & K(4) & -\frac{R_{dc}}{L_{dc}} & 0 \\ K_{tq}\lambda_{dr} & -K_{tq}\lambda_{qr} & 0 & 0 & 0 & 0 & 0 & 0 \end{bmatrix}$$

$$x = [\lambda_{qs} \quad \lambda_{ds} \quad \lambda_{qr} \quad \lambda_{dr} \quad v_{qs} \quad v_{ds} \quad i_{dc} \quad \omega_{me}]^t$$

$$B = \begin{bmatrix} 0 & 0 & 0 & 0 & 0 & 0 & \frac{1}{L_{dc}} & 0 \\ 0 & 0 & 0 & 0 & 0 & 0 & 0 & -\frac{P}{2J} \end{bmatrix}^t$$

$$u = [v_{dc} \quad T_l]^t$$

This state equation has been arranged in such a way that it is valid for all states. For different states, only the switching coefficients *K(1)* to *K(4)* in the equation need to be modified. Therefore, simulation complexity is substantially reduced. Furthermore, this state equation is already expressed in a stator reference frame and thus time domain waveforms can be directly obtained by using any numerical integration method without further transformations. As mentioned earlier, the operation of the inverter can be divided into six distinct states. Each state corresponds to a unique pair of on state thyristors. The definition of each state is given in Table 3.1.

Table 1: Switching States.

State	On-state Thyristors
1	T_1& T_2
2	T_2& T_3
3	T_3& T_4
4	T_4& T_5
5	T_5& T_6
6	T_6& T_1

The switching coefficients for different states can be derived as follows. For example, in state 5, T_5 and T_6 are turned on, and the following equations can be obtained.

$$i_{ai} = 0 \quad (2)$$
$$i_{bi} = -i_{dc} \quad (3)$$
$$i_{ci} = i_{dc} \quad (4)$$
$$v_{cb} = v_{cs} - v_{bs} \quad (5)$$

Applying 3ϕ to 2ϕ transformation matrix to Equations (2) – (5) gives

$$v_{cb} = \sqrt{3} v_{ds} \quad (6)$$
$$i_{qi} = 0 \quad (7)$$
$$i_{di} = \frac{2}{\sqrt{3}} i_{dc} \quad (8)$$

DC link voltage is expressed as

$$v_{dc} = L_{dc} \frac{di_{dc}}{dt} + R_{dc} i_{dc} + v_{cb} \quad (9)$$

Equation (6) when substituted in Equation (9) results

$$\frac{di_{dc}}{dt} = \frac{R_{dc}}{L_{dc}} i_{dc} - \frac{\sqrt{3}}{L_{dc}} v_{ds} + \frac{1}{L_{dc}} v_{dc} \quad (10)$$

Substitute Equation (7) and Equation (8) in stationary reference frame equation of Figure 5 and combine Equation (10) with Equation (1) in which the coefficient *K* is given as

$$K(1) = 0, \quad K(2) = \frac{2}{\sqrt{3}c}, \quad K(3) = 0, \quad K(4) = \frac{\sqrt{3}}{L_{dc}}$$

The coefficients *K(1)* to *K(4)* for different states are summarized in Table 2.

In this paper, a MATLAB s-function program codes are developed for the CSI-IM section. The s-function file is saved as an m-file. It contains the protocol in which Simulink can access information from MATLAB. So, this program was a combination of MATLAB m-file codes and Simulink blocks. With the complexity of large-size nonlinear models, such as Equation (1), it may be more efficient to use a set of differential equations written

in an m-file. These m-files will be accessed by Simulink through S-function block. Thus, this method mixes the advantages of an m-file which can be run directly by solvers such as ode45, with the graphical links to other Simulink blocks.

Table 2: Switching coefficients *K*.

State	*K(1)*	*K(2)*	*K(3)*	*K(4)*
1	$\frac{1}{C}$	$-\frac{1}{\sqrt{3}C}$	$-\frac{3}{2L_{dc}}$	$\frac{\sqrt{3}}{2L_{dc}}$
2	0	$-\frac{2}{\sqrt{3}C}$	0	$\frac{\sqrt{3}}{L_{dc}}$
3	$-\frac{1}{C}$	$-\frac{1}{\sqrt{3}C}$	$\frac{3}{2L_{dc}}$	$\frac{\sqrt{3}}{2L_{dc}}$
4	$-\frac{1}{C}$	$\frac{1}{\sqrt{3}C}$	$\frac{3}{2L_{dc}}$	$-\frac{\sqrt{3}}{2L_{dc}}$
5	0	$\frac{2}{\sqrt{3}C}$	0	$-\frac{\sqrt{3}}{L_{dc}}$
6	$\frac{1}{C}$	$\frac{1}{\sqrt{3}C}$	$\frac{3}{2L_{dc}}$	$-\frac{\sqrt{3}}{2L_{dc}}$

2.4 Control Section:

The simulation for the control circuit is relatively simple. The dynamic performance of any control scheme can be described by a set of differential equations presented in Bin Wu (1994). These equations can be solved numerically. As an example, consider the control circuit of the drive shown in Figure 1. It is assumed that both the compensators are of PI type, that is,

$$V_\alpha = \left(K_i + \frac{K_i}{\tau_i s}\right)\left(I_f^* - I_f\right) = K_i\left(I_f^* - I_f\right) + V_{pii} \tag{11}$$

Where

$$V_{pii} = \frac{K_i}{\tau_i s}\left(I_f^* - I_f\right) \tag{12}$$

and

$$I_f^* = \left(K_s + \frac{K_s}{\tau_s s}\right)\left(\omega_m^* - \omega_{mf}\right) = K_s\left(\omega_m^* - \omega_{mf}\right) + I_{pis} \tag{13}$$

Where

$$I_{pis} = \frac{K_s}{\tau_s s}\left(\omega_m^* - \omega_{mf}\right) \tag{14}$$

The outputs of the current and speed feedback filters can be expressed as

$$I_f = \frac{K_{cs}}{1+\tau_{if} s} I_s \tag{15}$$

and

$$\omega_{mf} = \frac{K_{ss}}{1+\tau_{sf} s}\omega_m \tag{16}$$

Equations (12), (14) - (16) can be expressed in matrix form:

$$p\begin{bmatrix} v_{pii} \\ i_f \\ i_{pis} \\ \omega_{mf} \end{bmatrix} = \begin{bmatrix} 0 & -\frac{K_i}{\tau_i} & \frac{K_i}{\tau_i} & -\frac{K_i K_s}{\tau_i} \\ 0 & -\frac{1}{\tau_{if}} & 0 & 0 \\ 0 & 0 & 0 & -\frac{K_s}{\tau_s} \\ 0 & 0 & 0 & -\frac{1}{\tau_{sf}} \end{bmatrix}\begin{bmatrix} v_{pii} \\ i_f \\ i_{pis} \\ \omega_{mf} \end{bmatrix} + \begin{bmatrix} \frac{K_i K_s}{\tau_i}\omega_m^* \\ \frac{K_{cs}}{\tau_{if}} i_s \\ \frac{K_s}{\tau_s}\omega_m^* \\ \frac{K_{ss}}{\tau_{sf}}\omega_m \end{bmatrix} \tag{17}$$

In this paper, a MATLAB s-function program is developed for the control section. The input parameters passed to the simulation program for the control circuit are the speed reference ω_m^* , the actual machine speed ω_m and stator current i_s . The output parameters brought back to the power circuit are the delay angle α and stator frequency ω_s which is the sum of the motor speed and rotor (slip) frequencyω_r. This rotor frequency is set at the rated value of the IM.

2.5. Simulation Implementation of Vector Based V/F Control:

In this section, the simulation implementation procedures are described in detail. The developed MATLAB simulation programs are simulated using MATLAB software. The rectifier section is realized with the help of a MATLAB function. It is a user defined function; the parameters incorporated to the function for evaluation are frequency, time instant, firing angle, RMS value of input line voltage. After the evaluation, it brings back the instantaneous value of dc link voltage. The Simulink implementation is shown in Figure 6. The simulation results are already shown in Figure 3.

The CSI-IM section is realized by means of S-Function. It is a user defined block. In these blocks, the code that defines the model in state Equation (1) can be written. In the code, the number of inputs and outputs are defined like the states and the state space equations of the system. To solve Equation (1), an mfile program is developed. This csiimvf sfcn.m can be drafted from sfunction Simulink block. For the motor parameters, the sfcn.m file calls another mfile which has the motor parameters. The Simulink implementation of CSI-IM section is shown in Figure 7. The control section can also be realized with a similar fashion. In another way the control voltage V_α Equation (11) can be obtained by using constant, transfer function blocks.

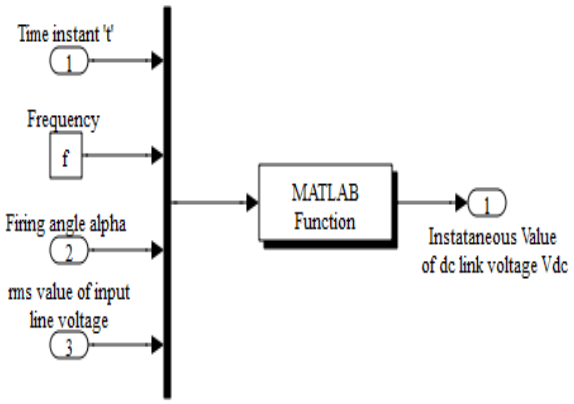

Fig. 6: Simulink implementation of rectifier section.

A simplified simulation procedure is summarized as follows.

1. Initialization.
2. Call rectifier subroutine.
3. Determine current state according to the switching pattern.
4. Select coefficient *K*from Table 2.
5. Solve state equation (2.1)for the inverter-motor section.
6. Calculate the stator frequency $\omega_s = \omega_r + \omega_{me}^*$
7. Solve equation (2.11) for the control Section.
8. Calculate the delay angle α
9. Go back to Step 2if the required ending time for simulation is not reached.

The proposed CSI fed IM control algorithm is validated by simulation. The IM parameters are obtained from Mummadi Veerachary (2002). The control system parameters are derived from Bin Wu (1994). The Simulink circuit diagram of vector based V/f controlled CSI fed IM drive shown in Figure 8 is simulated. The open loop and closed loop speed control and dynamic performance of the drive are obtained for different inverter switching frequency and are presented in the next section.

The developed vector based V/f control model shown in Figure 8 is simulated to compare the performance of the open loop and closed loop control modes of the CSI fed IM drives system. The following figures show the steady state and dynamic waveforms of the drive system at three different stator frequencies.

Figure 9 and 10 shows the dynamic performance of the drive system operated at the stator frequency of 50 Hz in open loop and closed control. The step command of the motor torque is changed from no load to full load at a step time of 2 seconds. Due to this step command, there is a dip in motor speed at 2 seconds. After a few milliseconds, the motor speed raises to its reference speed.

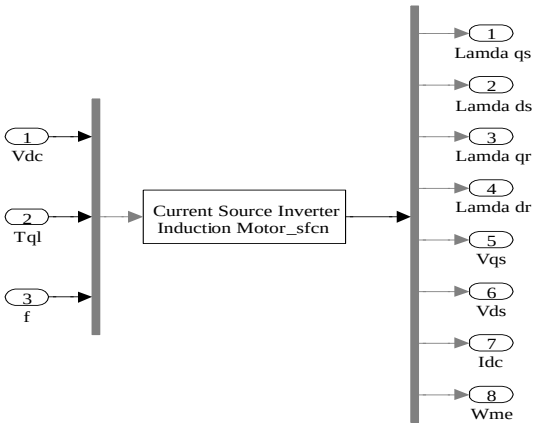

Fig. 7: Simulink implementation.

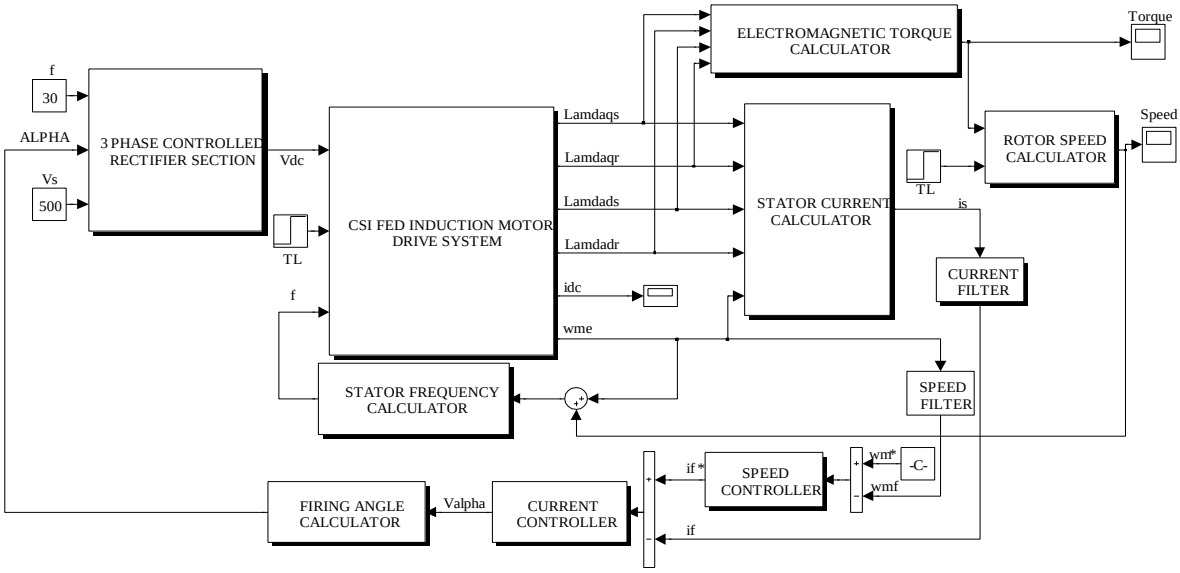

Fig. 8: Simulink implementation of V/f control method.

3. Simulation Results:

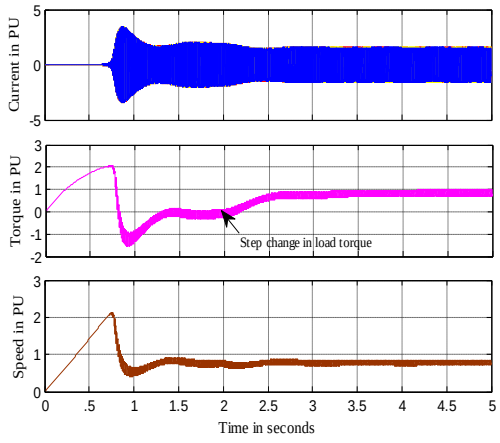

Fig. 9: Dynamic performance of the drive at 50 Hz in Open loop control.

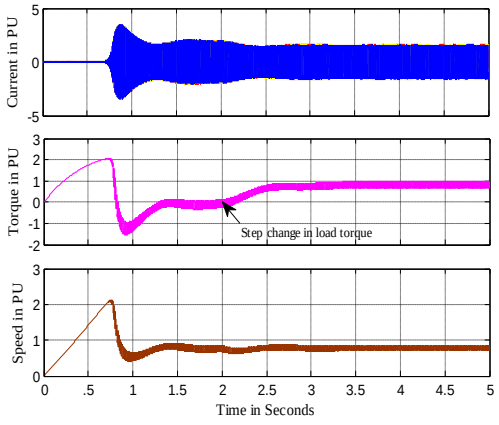

Fig. 10: Dynamic performance of the drive at 50 Hz in Closed loop control.

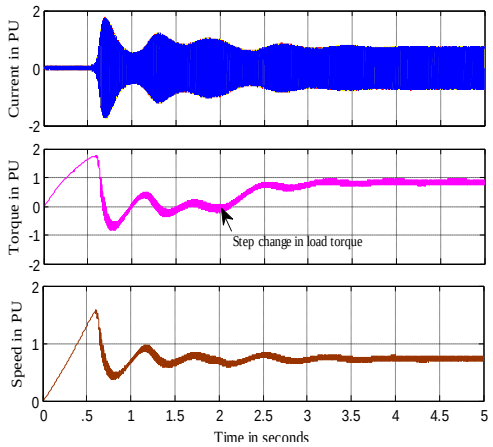

Fig. 11: Dynamic performance of the drive at 30 Hz in Open loop control.

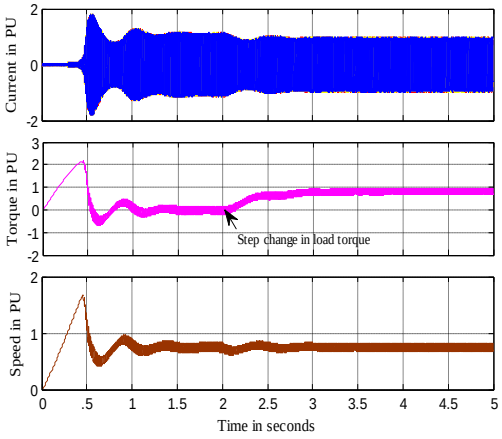

Fig. 12: Dynamic performance of the drive at 30 Hz in Closed loop control.

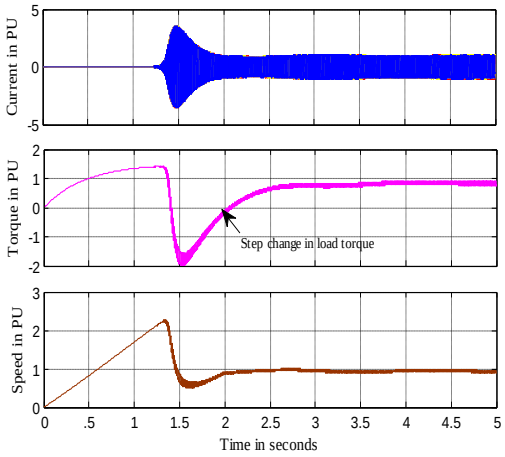

Fig. 13: Dynamic performance of the drive at 60 Hz in Open loop control.

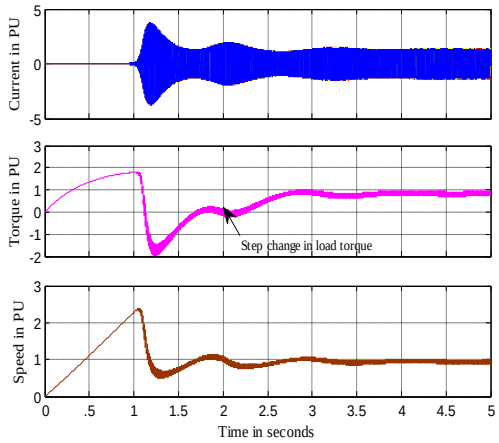

Fig. 14: Dynamic performance of the drive at 60 Hz in Closed loop control.

Similarly, Figure 11 and 12 shows the dynamic performance of drive system operated at the stator frequency of 30 Hz (below rated frequency) in open loop and closed loop controls and Figure 13 and 14 shows the dynamic performance of drive system operated at the stator frequency of 60 Hz (above rated frequency) for the full load step command of motor torque at 2 seconds. In closed loop control mode operation, 50% of torque and speed ripples (pulsations) are reduced compared to the open loop control mode of operation. Figure 15 (a), (b), (c) shows the steady state waveforms of the motor currents when the drive system is operated at 30 Hz, 50 Hz and 60 Hz in closed loop control. When the drive is operated at low frequency and open loop control, switching transients are more, resulting in high torque pulsations Figure 15 (a). In Figure 15 (b) and (c) due to closed loop control and high operating frequency, the motor current waveforms are almost sinusoidal in nature and the switching transients are almost eliminated. The tabular presentation of the simulation results are shown in the Tables 3 and 4.

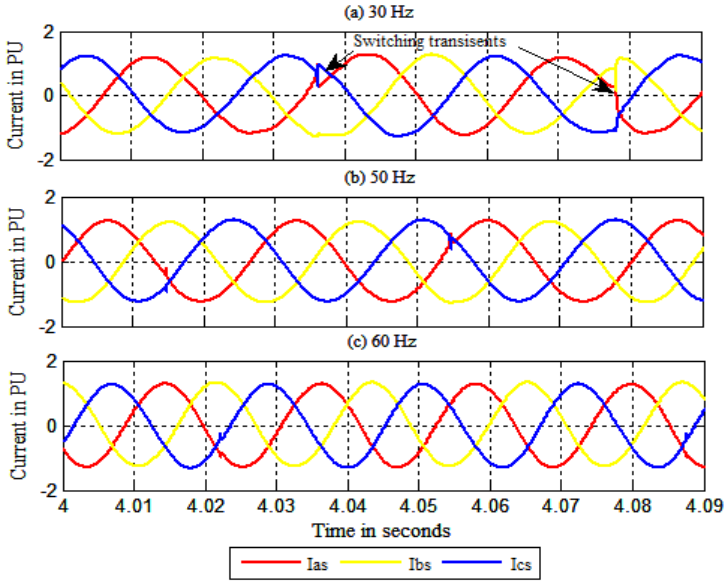

Fig. 15: Steady state currents of closed loop drives after step change in load torque (a) at 30 Hz (b) at 50Hz and (c) at 60 Hz.

Table 3: Dynamic performance of V/f controlled drive at 30 Hz.

Motor parameters	OPEN LOOP CONTROL MODE					
	Constant load			Full load		
	t_r(ms)	t_s (ms)	M_p (%)	t_r(ms)	t_s (ms)	M_p (%)
Stator current	216	1173	109	290	1172	149
Motor speed	749	1173	100	630	1172	122
	CLOSED LOOP CONTROL MODE					
	Constant load			Full load		
	t_r(ms)	t_s (ms)	M_p (%)	t_r(ms)	t_s (ms)	M_p (%)
Stator current	120	1065	14	43	1100	180
Motor speed	527	1065	106	43	1100	114

Table 4: Dynamic performance of V/f controlled drive at 60 Hz.

Motor parameters	OPEN LOOP CONTROL MODE					
	Constant load			Full load		
	t_r(ms)	t_s (ms)	M_p (%)	t_r(ms)	t_s (ms)	M_p (%)
Stator current	197	1032	139	252	1032	587
Motor speed	136	1032	126	114	1032	152
	CLOSED LOOP CONTROL MODE					
	Constant load			Full load		
	t_r(ms)	t_s (ms)	M_p (%)	t_r(ms)	t_s (ms)	M_p (%)
Stator current	328	996	78	138	1123	665
Motor speed	109	996	136	46	1123	137

RESULTS AND DISCUSSION

Alfredo Munoz-Garcia (1998) presented a new open loop constant V/f control method for VSI fed IM and concluded that it can be easily implemented in the existing V/f drives by modifying the software. In this paper, a vector based V/f control method for CSI fed IM drive is developed and simulated using MATLAB software. Simple control programs are developed for different sections in the drive system to avoid complexity in the simulation process. The developed MATLAB programs combine the advantages of an m-file which can be run directly by solvers such as ode45 with the graphical links to other Simulink blocks. These programs can modify any kind of drive system. The drive control system is developed using the model presented in Bin Wu (1994).The PWM switching states are derived using switching patterns presented in Bin Wu et al (1992). Dynamic performances are obtained for both open loop and closed loop operation modes of the drive system. It is evident from Tables 3 and 4 that during closed loop control mode operation with higher stator frequencies, there is a considerable improvement of the dynamic response in speed and current in terms of rise time and settling time. When the drive is operated at low frequency with open loop control, switching transients are more as shown in Figure 15 (a), resulting in high torque pulsations. When the drive is operated in closed loop control

and high frequency, the motor current waveforms are almost sinusoidal; the switching transients are almost eliminated as seen in Figure 15 (c).

5. Conclusion:

This Paper contains a review of the theoretical concepts used in the simulation and implementation of vector based V/f control of CSI fed IM drives. It is the simplest motor drive since it requires no parameter knowledge and is essentially an open-loop drive. The typical control structures are presented in a synthetic form. A simplified computer simulation procedure is introduced. To simplify the simulation process, different simulation algorithms are developed. The above sections elaborately described the D-Q axes model of IM with flux linkages as state variables especially for stability studies, different drive sections, implementation procedures, results and discussion.

The most important contributions in this paper are:

- Simplified programming codes for the rectifier section using MATLAB functions are developed.
- MATLAB S-function programming codes with Simulink blocks for CSI-IM drive section are developed and implemented.
- The Sim-power system Simulink blocks are developed to solve the state equations of the control section.

Results are presented in simulation waveforms and tabular forms.

REFERENCES

Ahmet M. Hava, 1999. J. Seung-Ki Sul, A.Russel Kerkman and Thamas Lipo, "Dynamic Over modulation Characteristics of Triangle Intersection PWM Methods" IEEE Trans. Ind. Appl., 35(4): 896-907.

Aleksandar Nikolic and Borislav Jeftenic, 2008. "Different Methods for Direct Torque Control of Induction Motor Fed from Current Source Inverter", Wseas Trans. Circuits and Systems, pp: 738-748.

Aleksandar Nikolic and Borislav Jeftenic, 2004. "Speed Sensorless Direct Torque Control Implementation in a Current Source Inverter Fed Induction Motor Drive", 35th Annul IEEE Power Electronics Specialists Conference, Aachen, Germany, pp: 2843-2848.

Alfredo Munoz-Garcia, A. Thomas Lipo and W. Donald Novotny, 1998. "A New Induction Motor V/f Control Method Capable of High-Performance Regulation at Low Speeds", IEEE Trans. Ind. Appl., 34(4): 813-821.

Babaei, M. and H. Heydari, 2010. "Direct Torque Control of Pulse Width Modulation Current Source Inverter-fed Induction Motor by Novel Switching Method", Taylor & Francis: Electric Power Components and Systems, 38: 514-532.

Bimal K. Bose, 2002. Modern Power Electronics and AC Drives, Prentice Hall, New Jersy.

Bin wu, 2006. "High-Power Converters and AC Drives", IEEE Press, A John Wiley & Sons, Inc., Publication.

Bin Wu, B. Shaahi Dewan and R. Gordon Slemon, 1992. "PWM CSI Inverter Induction Motor Drives", IEEE Trans. Ind. Appl., 28(1): 64-71.

Bin Wu, S.B. Dewan and G.R. Slemon, 1994. "Eigenvalue Sencitivity Analysis of GTO-CSI Induction Machine Drives", IEEE Trans. Ind. Appl., 30(3): 767-775.

Blaschke, F., 1971. "A new method for the structural decoupling of A.C. induction machines", in Conf. Rec. IFAC, Duesseldorf, Germany, pp: 1-15.

Blaschke, F., 1972. "The principle of field-orientation as applied to the transvector closed-loop control system for rotating-field machines", *Siemens Rev*., 34: 217-220.

Mummadi Veerachary, 2002. "Optimal Control Strategy For A Current Source Inverter Fed Induction Motor", Elsevier: Computers and Electrical Engineering, 28: 255-267.

Yidan Li, DeweiXu and Bin Wu, 2004. "Real-Time Simulator for Medium Voltage Drives Fed by Current Source Inverter," 35th Annual IEEE Power Electronics Specialists Conference, Germany, pp: 3547-3552.